EPJ Nuclear Sci. Technol. **5**, 15 (2019)

https://doi.org/10.1051/epjn/2019026

EPJ Nuclear Sciences & Technologies

Available online at:
https://www.epj-n.org

REGULAR ARTICLE

OPEN ACCESS

Breed-and-burn fuel cycle in molten salt reactors

Boris Hombourger[1,2,*], Jiři Křepel[1], and Andreas Pautz[1,2]

[1] Paul Scherrer Institut, Nuclear Energy and Safety Division, Laboratory for Scientific Computing and Modelling, 5232 Villigen PSI, Switzerland
[2] École Polytechnique Fédérale de Lausanne, Laboratory for Reactor Physics and Systems Behavior, 1015 Lausanne, Switzerland

Received: 1 April 2019 / Received in final form: 1 July 2019 / Accepted: 12 August 2019

Abstract. The operation of a reactor on an open but self-sustainable cycle without actinide separation is known as breed-and-burn. It has mostly been envisioned for use in solid-fueled fast-spectrum reactors such as sodium-cooled fast reactors. In this paper the applicability of breed-and-burn to molten salt reactors is investigated first on a cell level using a modified neutron excess method. Several candidate fuel salts are selected and their performance in a conceptual three-dimensional reactor is investigated. Chloride-fueled single-fluid breed-and-burn molten salt reactors using enriched chlorine are shown to be feasible from a neutronics and fuel cycle point of view at the cost of large fuel inventories.

1 Introduction

Currently, the vast majority of existing reactors is composed of reactors operating on an open uranium fuel cycle that, on the one hand, cannot achieve net breeding of fissile material, and on the other hand have limited discharge burn-ups (up to approximately 5% fissions per initial metal atom (FIMA)). These reactors therefore need a fissile fuel make-up using some degree of uranium enrichment, as well as release important amounts of unfissioned actinides to the waste stream, resulting in their arguably poor fuel efficiency (approximately 0.05% of mined natural uranium).

Conventional breeder reactors alleviate this problem by converting more of their fertile feed into fissile material (positive breeding gain) and adopting fuel recycling to recover fissile material and remove fission product (FPs) from the nuclear fuel, thereby substantially increasing their fuel efficiency. However, reprocessing comes at an increased fuel cycle cost as well as an increased proliferation risk if fissile material is separated during processing.

Instead, the idea of instead operating breeder reactors on an open cycle without actinide separation and discharging the fuel at a sufficiently high burn-up for the reactor to remain self-sustainable, termed breed-and-burn (BNB), has been considered. While it represents an interesting compromise between both previous cases, the technological challenge of reaching high burn-ups has proved problematic due to maximum cladding fluence limitations. The stringent requirements on the neutron economy needed for breeding implies it has mainly been considered for implementation in sodium-cooled fast reactor (SFRs) but also in other fast reactors.

However, implementing some form of BNB cycle in Molten salt-fueled reactors[1] (MSRs) could provide an alternative answer to the challenges encountered in solid-fuel fast reactors. Indeed, externally-cooled MSRs use their molten salt fuel as coolant and therefore have no cladding material in the core. Additionally, liquid fuels are not embrittled by radiation and can thus theoretically remain in core indefinitely.

In this work, the feasibility of implementing a BNB cycle in MSRs is investigated from a neutronics and fuel cycle point of view. First, the concept of BNB is discussed in more details in Section 2. Mathematical models used to investigate performance of various potential fuels are explained in Section 3. The performance of several candidate salts is evaluated for BNB on a zero-dimensional level in Section 4. Finally, potential reactor charateristics of three-dimensional, finite core designs are computed and compared in Section 5.

2 Breed-and-burn fuel cycle

BNB reactors are an old idea dating back to a least the time of the Second International Conferences on the

[1] In this paper, the acronym molten salt reactor (MSR) only refers to molten salt-fueled reactors and not molten salt-cooled reactors which are normally included under the MSR umbrella.

* e-mail: boris.hombourger@protonmail.com

Peaceful Uses of Atomic Energy [1] during which Feinberg highlighted the practicality of not having to reprocess the fuel of a fast reactor during the cycle. It has been investigated by researchers such as Klaus Fuchs [2], which investigated the possibility of an homogeneous BNB reactor and Edward Teller [3] which brought the idea of a gas-cooled and thorium-fueled BNB reactor. Japanese researchers [4] have brought the idea of a fission wave propagating uniaxially to avoid the radial redistribution of heat sources in the core which complicates core design. Most recently the company TerraPower has been developing a sodium-cooled BNB reactor since 2006 [5]. Interested readers are referred to a recent article [6] which reviews the concept in many more details.

Fundamentally, a BNB reactor is a reactor capable of operating on a fertile-only feed in an open cycle without actinide separation from its discharged fuel, by opposition to a classical breeder reactor, sometimes called *seed-and-blanket*, in which the fissile elements are mostly bred in a dedicated part of the reactor (blanket) which is reprocessed and its actinides separated at relatively low discharge burn-up to produce new fuel with a higher concentration of fissile elements. It must be mentioned that there are two main types of BNB reactors:

- traveling wave reactor (TWRs), in which a fission wave propagates in a static fuel, and
- standing wave reactor (SWRs), in which the fuel is moved and the flux does not propagate.

While TWRs are simpler because it is not be necessary to shuffle fuel in the core, the technological challenges posed by the fluences necessary to achieve BNB are substantial. In SWRs, the fuel can be moved to regions where it is the most effective depending on its burn-up: for example, highly burnt fuel need not be in a high flux region as it will be a net neutron absorber. Therefore, cladding fluence can be decreased compared to the TWR. Moreover, in the case of strictly static fuel, inhomogeneity of the neutron flux due to the finite size of the core leads of a loss of efficiency in the fuel because of lower burn-up at the extremities of fuel assemblies. It has been proposed to make the fuel move radially as well as axially (3D shuffling) to alleviate this limitation [7].

The necessity of conserving a positive breeding gain without actinide separation applies stringent requirements on the neutron economy of the reactor. Therefore, the design space is generally limited to reactors possessing:

- a hard neutron spectrum to limit parasitic neutron captures on structural materials and FPs,
- a large core to lower neutron leakage, usually coming at the cost of worsened safety parameters (such as void reactivity worth) in liquid metal fast reactors,
- an actinide-dense fuel form to further improve both previous factors.

Technologically, one of the most limiting factors is the maximum allowable fluence on the cladding because its integrity must be guaranteed with sufficient safety margins. Some concepts lead to displacement per atom (dpa) values in the cladding tubes of up to 1200 dpa, while various optimization measures can be taken to bring this value down to at least 350 dpa, which is still higher than the 200 dpa reference cladding materials such as HT9 have been tested up to [7]. For example, fuel re-cladding can be considered, with some associated cost and technical complications.

However, a third type of BNB can be conceived when implemented in an externally-cooled MSR in which the primary coolant is the fuel salt, which would bring an alternative. It has the advantages that:

- the fuel being homogeneously mixed, there is no loss of fuel efficiency due to flux inhomogeneities,
- the absence of cladding tubes implies that fuel residence time would not be limited by fluence considerations (while remaining a limiting factor for the vessel lifetime, however without substantial differences compared to other fast-spectrum MSR concepts),
- the void reactivity will remain negative in the case of a fast-spectrum system as long as provisions are made for the salt to be able to expand freely upon heating up,
- the properties of molten salts should allow higher outlet temperatures than are possible in a liquid metal-cooled reactor,
- insoluble and volatile FPs will naturally be removed from a molten salt mixture, which can be enhanced by He bubbling, as is foreseen in many MSR designs.

This work builds on preliminary findings on the feasibility of BNB in MSRs [8–10]. Additionally, [11] investigated the feasibility of implementing a BNB cycle in an internally-cooled MSR in which the fuel is contained in separate tubes and cooled by another salt, based on Moltex energy's stable salt reactor concept [12]. This different implementation was not explicitely considered in the present work, however, as it is closer to the implementation of BNB in a solid-fuel reactor.

3 Model of a breed-and-burn molten salt reactor

Quantities of interest in the evaluation of the performance of candidate fuels or geometries for use in BNB reactors include the minimum and maximum burn-ups achievable, as well as the resulting multiplication factors.

The neutron excess method [13,14] uses a simple neutron balance for a unit element of fuel to compute the net number of neutrons produced as function of time or burn-up, based on the net number of neutrons produced after a given time in flux, which in the zero-dimensional case is given by:

$$P(t) = \int_0^t \overline{\nu} F(\theta) - A(\theta)\, \mathrm{d}\theta = \int_0^t \left[\overline{\nu}\Sigma_{\mathrm{f}}(\theta) - \Sigma_{\mathrm{a}}(\theta)\right] \phi(\theta)\, \mathrm{d}\theta \tag{1}$$

in which P is the net number of neutrons produced, $\overline{\nu}$ the average number of neutrons per fission, F and A the

fission and absorption rates, and Σ_f and Σ_a the fission and absorption macroscopic cross-sections, and ϕ the neutron flux. The evolution of rates and cross-sections as function of time can be obtained by depleting a unit cell of the configuration of interest.

While this description is adequate to model a fuel element of a static-fuel reactor, in an externally-cooled (circulating fuel) MSR the fuel is constantly mixed. At discharge, the fuel will be a mixture of volumes that have spent different amounts of time in the core and therefore have been exposed to different fluences, unlike the fuel of a solid-fuel reactor which will have spent exactly the same amount of time in the core.

This difference can be modeled using the concept of residence time distribution (RTDs) of ideal reactors [15]. One can define an exit age distribution $E(t)$ describing the age (time spent in the reactor) of fuel taken from it and an internal age distribution $I(t)$ describing the age of the contents of the reactor. In the case of a so-called Plug Flow Reactor in which the contents do not mix and spend the same amount of time in the reactor, these are:

$$E_{\mathrm{SF}}(t) = \delta(t - \tau_{\mathrm{dis}}) \qquad I_{\mathrm{SF}}(t) = \frac{1}{\tau_{\mathrm{dis}}}\left[1 - H(t - \tau_{\mathrm{dis}})\right] \quad (2)$$

in which δ is the Dirac delta function and H the Heaviside step function. This RTD models that of a single-batch static-fuel (SF) reactor whose fuel is entirely discharged at a time τ_{dis}.

In the case of a MSR whose fuel is constantly discharged and replenished, the distribution is that of a so-called continuously-stirred tank reactor (CSTR) in which the mixed fuel (MF) is continuously mixed and discharged at a rate $\dot{v}$ from a total fuel volume V:

$$E_{\mathrm{MF}}(t) = \frac{\dot{v}}{V}\exp\left(-\frac{\dot{v}}{V}t\right) = \frac{1}{\tau}\exp\left(-\frac{1}{\tau}t\right)$$
$$I_{\mathrm{MF}}(t) = E_{\mathrm{MF}}(t) \quad (3)$$

in which the discharge cycle time $\tau = \frac{V}{\dot{v}}$ was defined, which is the time needed to discharge the whole fuel volume, and also the average residence time of a fuel element in the core, as will be shown later. It must be noted that the exit and internal distributions are equal since the contents of the reactor are supposed to be instantly and continuously mixed, therefore they have the same distribution. For comparison, the distributions are illustrated in Figure 1.

The RTDs can be used to derive average values pertaining to the reactor. For example, the average age of fuel at discharge $\overline{T}_{\mathrm{dis}}$ and in the reactor $\overline{T}_{\mathrm{in}}$ is given by:

$$\overline{T}_{\mathrm{dis}} = \int_0^\infty t\ E(t)\ \mathrm{d}t \qquad \overline{T}_{\mathrm{in}} = \int_0^\infty t\ I(t)\ \mathrm{d}t. \quad (4)$$

Using equation (2) into (4) yields, for a static-fueled reactor:

$$\overline{T}_{\mathrm{dis,SF}} = \int_0^\infty t\ \delta(t - \tau_{\mathrm{dis}})\ \mathrm{d}t = \tau_{\mathrm{dis}}$$
$$\overline{T}_{\mathrm{in,SF}} = \int_0^\infty t\ \frac{1 - H(t - \tau_{\mathrm{dis}})}{\tau_{\mathrm{dis}}}\ \mathrm{d}t = \frac{\tau_{\mathrm{dis}}}{2}.$$

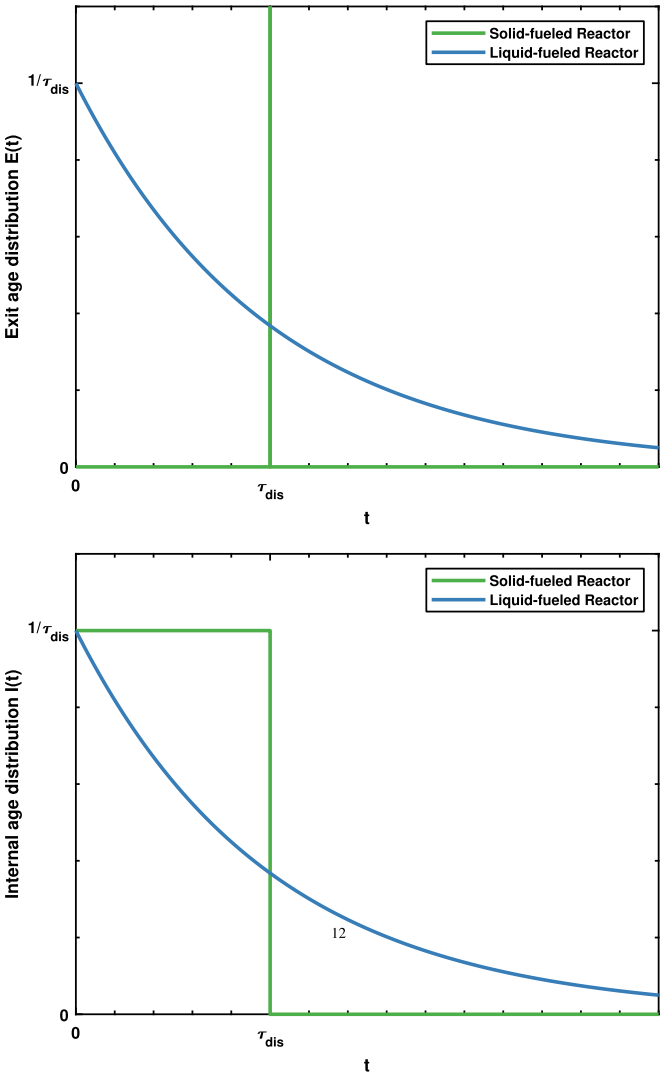

Fig. 1. Exit (top) and internal (bottom) residence time distributions for static- and mixed-fuel reactors of equal discharge and cycle times $\tau_{\mathrm{dis}} = \tau_{\mathrm{cycle}}$ as function of time.

While using (3) in (4) for a mixed-fuel reactor, one gets:

$$\overline{T}_{\mathrm{dis,LF}} = \int_0^\infty t\ \frac{1}{\tau}\exp\left(-\frac{1}{\tau}t\right)\ \mathrm{d}t = \tau \quad \overline{T}_{\mathrm{in,LF}} = \overline{T}_{\mathrm{dis,LF}} = \tau.$$

In both cases the results are quite trivial: in a static-fuel reactor the average age at discharge is the discharge time and the average age of fuel in the core is half of that, while in the case of mixed fuel the average ages are equal to the average residence time.

Nevertheless RTDs can be used to obtain the net neutron excess at discharge of the fuel as function of the discharge time τ:

$$P(\tau) = \int_0^\infty \mathrm{d}t\ E(t,\tau)\int_0^t \mathrm{d}\theta\ P(\theta). \quad (5)$$

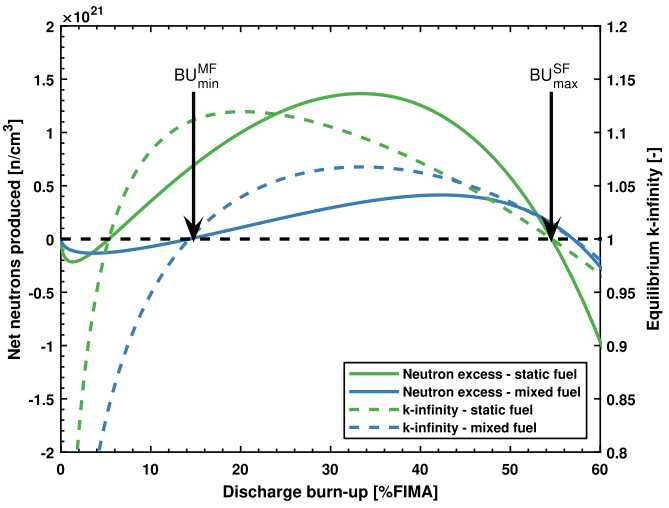

Fig. 2. Comparison of the neutron excess and equilibrium k_∞ using static-fuel and mixed-fuel distributions.

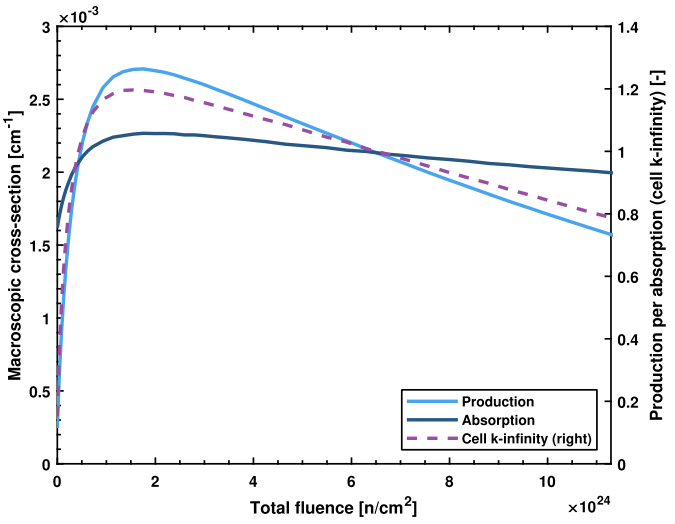

Fig. 3. Evolution of the neutron production ($\overline{\nu}\Sigma_\mathrm{f}$) and absorption macroscopic cross-sections as well as cell k_∞ as function of the total fluence for the NaCl−UCl_3 (68–32 mol%) case.

Computing (5) using (1) and (2) yield a trivial result:

$$P_\mathrm{SF}(\tau)=\int_0^\infty \mathrm{d}t\ \delta(t-\tau)\int_0^t \mathrm{d}\theta\ P(\theta)=\int_0^\tau \mathrm{d}\theta\ P(\theta)=P(\tau). \tag{6}$$

Equation (6) yields the trivial result that for a static-fuel reactor the net number of neutrons produced at discharge of the fuel is given by $P(\tau)$. However, in the case of a mixed-fueled reactor, one gets:

$$P_\mathrm{MF}(\tau)=\int_0^\infty \mathrm{d}t\ \frac{1}{\tau}\exp\left(-\frac{1}{\tau}t\right)\int_0^t \mathrm{d}\theta\ P(\theta).$$

The same process can be repeated for the number of neutrons absorbed A:

$$A(\tau)=\int_0^\infty \mathrm{d}t\ E(t)\int_0^t \mathrm{d}\theta\ A(\theta).$$

The equilibrium k_∞ can then be approximated by the ratio of neutrons produced to the neutrons absorbed:

$$k_\infty^\mathrm{eq}(\tau)=\frac{P(\tau)+A(\tau)}{A(\tau)}=1+\frac{P(\tau)}{A(\tau)}. \tag{7}$$

The differences between static and mixed-fuel distributions can be further illustrated by comparing their neutron excess and k_∞ distributions, as is done in Figure 2 using a NaCl−UCl_3 salt. The minimum and maximum burn-ups are given by

$$P(\mathrm{BU}_\mathrm{min})=P(\mathrm{BU}_\mathrm{max})=0$$

and are also visibly those point at which

$$k_\infty(\mathrm{BU}_\mathrm{min})=k_\infty(\mathrm{BU}_\mathrm{max})=1.$$

It can be noticed that in the case of the mixed-fuel distribution, the minimum discharge burn-up is higher than that of the static-fuel one, due to the fact that in a mixed-fuel core the youngest fuel (containing fissile isotopes) is already partially discharged due to mixing. On the other hand the maximum burn-up achieved in the static-fuel case is slightly lower due to the fact that in a mixed-fuel core the oldest fuel is also partially removed and replaced by fertile isotopes.

To test the method, several test salts whose characteristics are detailed in Section 4 were computed using this model and the EQL0D procedure for the cell calculations and discrete equilibrium points at fixed discharge rates (and thus burn-ups) were calculated using EQL0D as well.

The EQL0D procedure is a MATLAB®- and Serpent-based burn-up calculation tool with specific features for the simulation of MSR fuel cycles [16]. It uses the Serpent Monte-Carlo code [17] to obtain and update neutron reaction rates then used by the MATLAB® script to compute fuel evolution using the Chebyshev Rational Approximation Method (CRAM, [18]) and criticality. EQL0D can perform the necessary changes to fuel composition (removal of FPs, refueling, criticality control by composition adjustments, etc.) in a batch-wise or continuous (on-line) manner to simulate various fuel cycles. Finally, it possesses both standard finite-step burn-up and equilibrium search modes. In the calculations shown in this paper, insoluble and volatile FPs are removed with a 30 s removal time.

First, the evolution of unit cells containing the evaluated salts is computed using the EQL0D by burning them from 0% FIMA to approximately 100% FIMA at constant flux in sufficiently fine time-steps to obtain a good approximation of continuous data. The reaction rates as function of fluence are then used in conjunction with the model of (7) to obtain a prediction of the equilibrium k_∞ values as function of discharge rate (and thus, burn-up). An example of the evolution of the neutron production ($\overline{\nu}\Sigma_\mathrm{f}$) and absorption macroscopic cross-sections as well as the cell k_∞ are given in Figure 3.

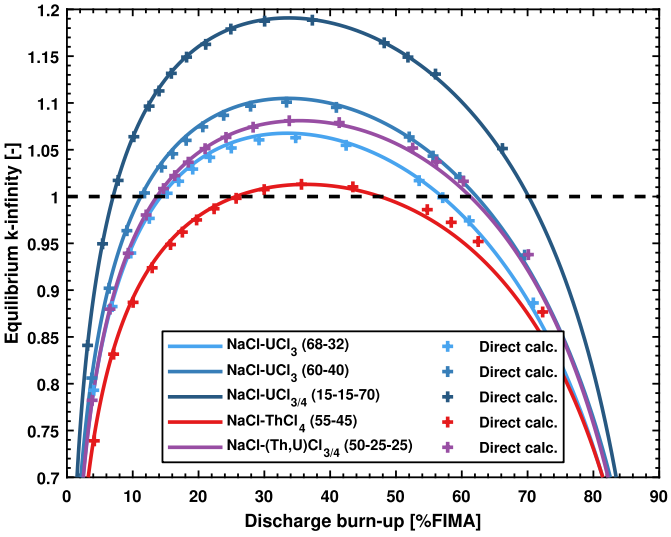

Fig. 4. Evaluation of the k_∞ at equilibrium using direct calculation (crosses) and the neutron excess method (lines).

For comparison purposes, individual equilibrium calculations using EQL0D are then carried out by selecting several arbitrary discharge rates, and the same unit cells are then iteratively burned and refueled until equilibrium is reached and both the fuel composition and cell k_∞ value do not vary any more. These point values obtained by direct calculation can then be compared to the continuous values predicted by the model. The comparison of the results obtained by these two methods can be made using Figure 4.

The agreement is arguably satisfactory for scoping studies, although it should be noticed that the method seems to slightly underestimate the k_∞ at equilibrium for Th-containing salts.

4 Fuel salt mixture selection

In this section, several candidate salts and configurations were evaluated for BNB. First, the candidate salts and their properties such as melting point and density are introduced and the way they were derived is explained. Afterwards, results pertaining to fluoride salts, in a moderated and non-moderated configuration, are presented. Finally, the results pertaining to chloride salts are presented, with a focus on the enrichment level of the chlorine isotopes.

4.1 Candidate salts and properties

Selection of a fuel salt mixture in MSRs is constrained by several requirements, including:

- low melting point: melting temperatures below 500 °C are usually favored, while melting temperatures below 550 °C are often considered acceptable,
- low capture cross-section for salts intended for thermal-spectrum MSRs,
- low scattering for salts intended for fast-spectrum MSRs,
- high solubility of actinides.

The last requirement is particularly relevant to BNB MSRs due to the necessity to minimize the total actinide inventory by decreasing the critical volume of salt.

The candidate salt mixtures were selected and their melting point deduced from phase diagrams in the literature. Their densities were computed using the additive molar volumes approximation [19], which gives for the density of a mixture ρ_{mix}:

$$\rho_{\text{mix}}(T) \approx \frac{\sum_i x_i M_i}{\sum_i x_i V_i(T)} \tag{8}$$

in which x_i is the molar fraction of component i, M_i is its molar mass, and $V_i(T)$ is its molar volume at the reference temperature. Linear interpolation can yield density approximations between two reference temperatures. Densities were computed using equation (8) and single-compound density data from [19] for fluoride salts and data from [20] for chloride salts. Since no data concerning Pu trifluoride and trichloride could be found, the density of the base salt was assumed. The melting points were approximated using phase diagrams from [21].

Table 1 provides a summary of pure compounds and potential fuel salts for a BNB MSR and their densities at 900 K. While chloride salt mixtures are obvious candidates due to their hard spectrum, simple fluoride salt mixtures were nonetheless investigated despite their relatively soft neutron spectrum.

A higher density of actinides improves a fuel salt's performance, such as the critical core size, by:

- decreasing the amount of captures on salt nuclides,
- decreasing the neutron leakage, and
- hardening the neutron spectrum.

The mixtures were therefore selected so as to maximize the actinide content with a maximum melting point of 500 °C if at all possible. Salt mixtures containing UCl_4 and $ThCl_4$ have noticeably lower melting points. However, it is expected that UCl_4 is unstable and corrosive at higher temperatures. Due to the large number of neutrons per fission of Pu isotopes, U-containing salts perform better than Th-containing ones. A compromise can thus be reached by mixing both fertile materials to optimize the melting point of the mixture. For this purpose the mixture $NaCl{-}ThCl_4{-}UCl_4$ (50–25–25 mol%) was investigated as well.

4.2 Fluoride salts

Fluoride salts have the advantage of having been much more investigated for use as fuel salts than chloride salts, as well as containing more actinides per unit volume than many chloride salts. Moreover, the softer neutron spectrum decreases leakage compared to the case of chloride salts. Additionally, they can be used in a thermal spectrum. In this section, they were evaluated for use in a

Table 1. Candidate fluoride and chloride fuel salts considered in this work and their properties.

Composition	[mol%]	Density [g cm^{-3}]		Melting
		Total	Act.	Temp.
$LiF-ThF_4$	72–28	4.59	2.84	565 °C
$LiF-UF_4$	73–27	4.67	2.89	500 °C
$NaCl-UCl_3$	68–32	3.32	1.66	520 °C
$NaCl-UCl_3$	60–40	3.64	1.97	590 °C
$NaCl-UCl_3-UCl_4$	15–15–70	3.64	2.22	500 °C
UCl_4-UCl_3	80–20	3.79	2.38	545 °C
UCl_4	100	3.56	2.20	590 °C
$NaCl-ThCl_4$	50–50	3.15	1.61	375 °C
$NaCl-ThCl_4-UCl_3$	50–25–25	3.16	1.67	500 °C
$ThCl_4$	100	3.82	2.33	770 °C

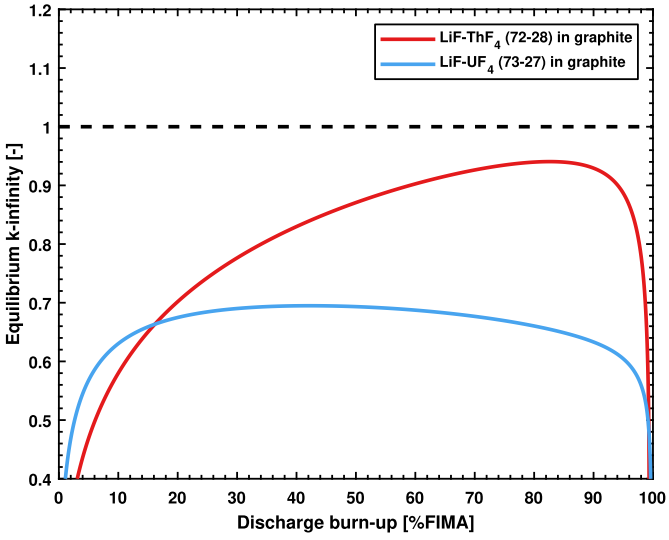

Fig. 5. Achievable equilibrium k_∞ as function of the discharge burn-up for fluoride salts in a graphite-moderated lattice.

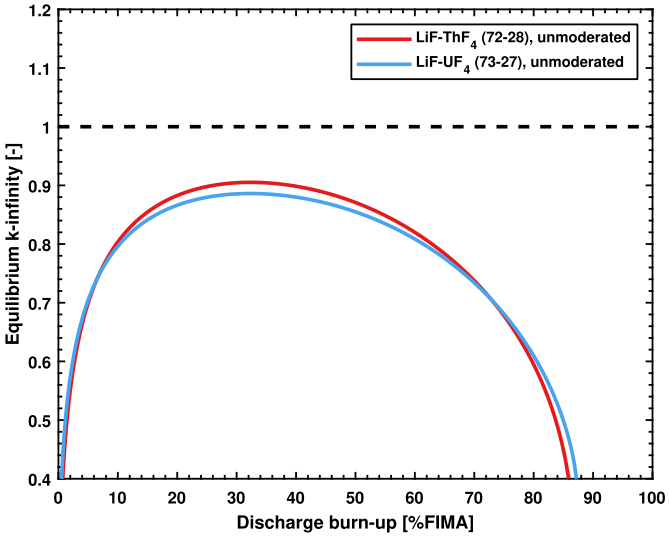

Fig. 6. Achievable equilibrium k_∞ as function of the discharge burn-up for fluoride salts in a fast spectrum.

graphite-moderated lattice and in a fast spectrum (no moderator).

4.2.1 Fluorides in a thermal spectrum

An hexagonal lattice composed of 10% fuel salt volume fraction in a cylindrical 1 cm channel and 90% volume fraction graphite with density $1.8\,\mathrm{g,cm^{-3}}$ and 2 appm natural Boron impurities was used to investigate the possibility of a graphite-moderated BNB MSR. The values were chosen as representative of a well-moderated graphite-moderated MSR, with the salt volume fraction comparable to that of the central zone (13%) of the 1971 molten salt breeder reactor concept [22].

The maximum k_∞ achievable at equilibrium computed using (7) and are depicted in Figure 5.

Neither salts reaches criticality in an infinite lattice, although LiF−ThF4 performs substantially better than $LiF-UF_4$ in a thermal spectrum.

4.2.2 Fluorides in a fast spectrum

The same fluoride salts were investigated in a fast neutron spectrum, with the results being depicted in Figure 6.

The difference between Th and U cycle is noticeably smaller than in a thermal spectrum. However, in both cases the fuel salts fails to reach net neutron generation and the equilibrium k_∞ remains below unity, precluding their use in a BNB reactor. It is therefore unlikely to obtain a BNB-capable reactor using fluoride salts.

4.3 Chloride salts

In [8], it was found that chlorine in chloride salts must be enriched in its ^{37}Cl isotope to obtain acceptable performance due to the large capture cross-section of ^{35}Cl. In the present paper, chloride-based salts were investigated using chlorine enriched to 100% ^{37}Cl (unless otherwise stated).

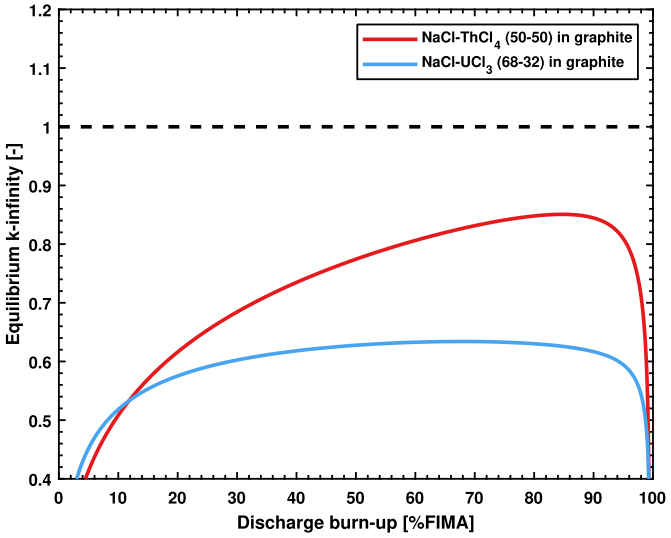

Fig. 7. Evaluation of the k_∞ at equilibrium of chloride salts in a thermal spectrum using the neutron excess method.

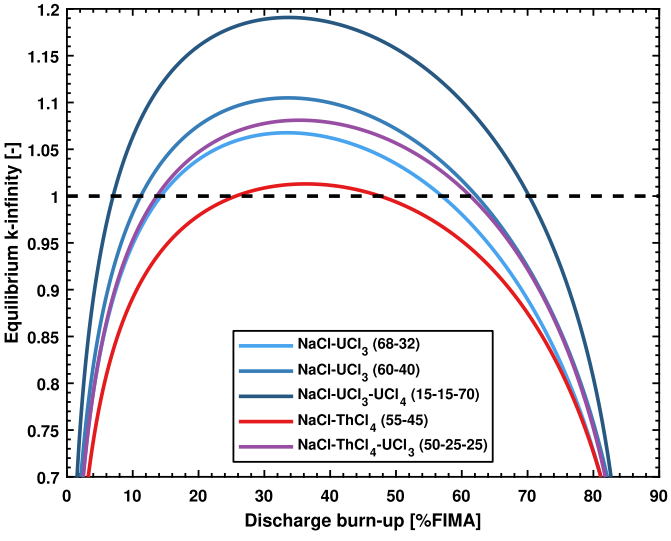

Fig. 8. Evaluation of the k_∞ at equilibrium of chloride salts in a fast spectrum using the neutron excess method.

4.3.1 Chlorides in a thermal spectrum

Similarly to the case of fluoride salts, chloride salts were tested in a graphite-moderated lattice. Since the chlorine is enriched in ^{37}Cl, the neutronic penalty of ^{35}Cl is minimized. The results are depicted in Figure 7.

However, like their fluoride counterparts, neither Th- or U-based chloride salts can reach criticality at equilibrium regardless of the discharge burn-up.

4.3.2 Chlorides in a fast spectrum

The results derived using the simplified method are reported graphically in Figure 8 as well as numerically in Table 2.

The results show that a pure Th-cycle BNB reactor is not practical due to the too low equilibrium k_∞ that is achievable. The pure U-cycle salts perform substantially better, with higher reactivity the higher their actinide density is, due to diminished parasitic captures and spectrum hardening. The mixed NaCl−$ThCl_4$−UCl_3 performs slightly better than NaCl−UCl_3 (68–32%mol.) due to the presence of Thorium which increases the maximum burn-up. The expected advantage is that the melting point of the NaCl−$ThCl_4$−UCl_3 mixture should be below 500 °C.

The maximum reactivity at equilibrium (and thus smallest core size) is obtained for fuel discharged at a burn-up in the range of 33 f to 37 FIMA for all salts. It is therefore possible to operate a chloride-fueled MSR on a BNB cycle.

Table 2. Zero-dimensional estimates of minimum, maximum burn-ups and burn-up at maximum reactivity achievable with enriched chloride salts.

Burn-up [FIMA]	Min.	Max.	Max. k_∞
NaCl−UCl_3 (68–32)	14.3	57	33.6
NaCl−UCl_3 (60–40)	11.2	62.3	33.8
NaCl−$ThCl_4$	25.7	47.6	36.1
NaCl−$ThCl_4$−UCl_3	13.7	61.3	35
NaCl−UCl_3−UCl_4	7	70.2	33.8

5 Performance comparison

Having ascertained the possibility of operating a chloride-fueled MSR on a BNB cycle in an infinite lattice, a more realistic three dimensional design can be investigated and optimized.

To minimize the physical size of the core, an adequate reflector material must first be selected; a challenging task due to the neutron transparency of chlorides salts which combine a low actinide density compared to solid fuels with a hard neutron spectrum, making finite-sized cores highly susceptible to neutron leakage and therefore quite large. In [9], several candidate reflector materials (Fe, Zr, Pb and ^{208}Pb) were evaluated and it was found that ^{208}Pb results in the lowest core size and inventory but with a marginal improvement over Pb, at the cost of isotopic enrichment. Therefore, Pb was selected in the present work as main reflector material. The Pb reflector was assumed to be sufficiently well cooled to remain in a solid state (melting point 327 °C), as molten Pb is incompatible with nickel alloys that are the reference container material for molten halide salts. PbO (melting point 888 °C) can be envisaged as an alternative with an expected minimal impact on the neutronics.

The four candidate salts that proved to be usable in a BNB MSR, that is, NaCl−UCl_3, NaCl−$ThCl_4$−UCl_3 (50–25–25) and NaCl−UCl_3−UCl_4 (15–15–70) were investigated at beginning-of-life (BOL), at equilibrium (EQL) and during the transition to said equilibrium and their performance compared.

All computations provided in this part were carried out using the EQL0D procedure and the Serpent 2.1.26 code [17] with the ENDF/B-VII.0 nuclear data library.

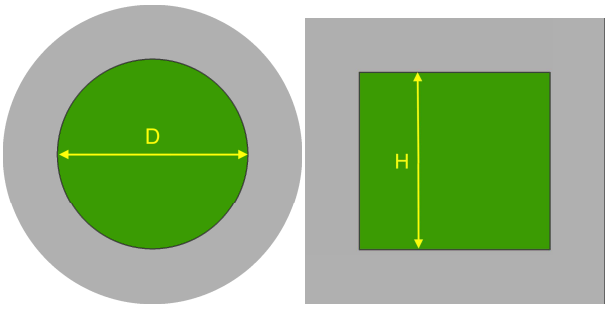

Fig. 9. Geometry of the cores investigated.

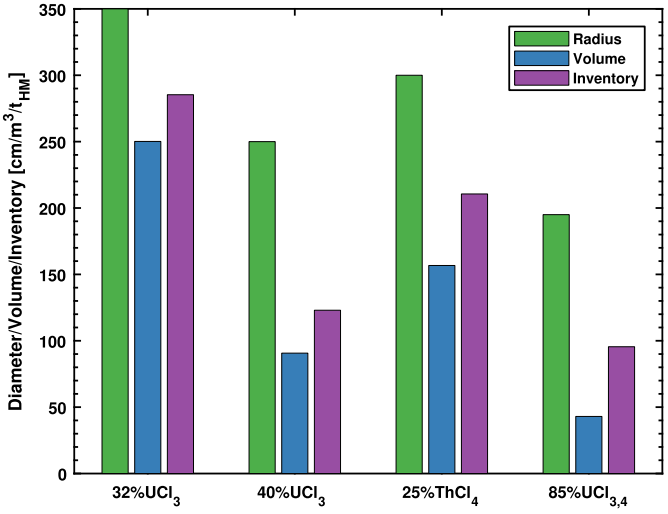

Fig. 10. Equilibrium core dimension for each selected candidate salts.

5.1 Geometry

The simplified geometry (see Fig. 9) used in this paper is that of a cylinder of optimum height-to-diameter ratio from diffusion theory:

$$\frac{H}{D} = \frac{\pi}{\sqrt{2}j_0} \approx 0.92374\ldots$$

in which j_0 is the first zero of the Bessel function of the first kind of first order J_0. A simple cylindrical vessel of 3 cm thickness made out of Hastelloy N and a 100 cm thick Pb reflector were further assumed, while the cooling loops were not accounted for, since they do not change the fuel cycle behavior of the reactor beyond increasing the salt inventory. This geometry is depicted in Figure 9.

5.2 Equilibrium core dimensions

For each possible salt, core dimensions critical at equilibrium at a discharge burn-up of maximum predicted k_∞ were computed. The calculated values for the diameters, core volume and heavy metal inventories are depicted in Figure 10.

The minimum values are obtained for the most actinide-dense salt, NaCl−UCl_3−UCl_4. An acceptably low volume and inventory is obtained with NaCl−UCl_3 (60–40), while other salts result in substantially large fuel volumes and inventories.

Table 3. Critical LEU and LWRPu fraction for each candidate salt.

^{235}U or Pu fraction	LEU	LWRPu
NaCl−UCl_3 (32–68)	10.65%	11.3%
NaCl−UCl_3 (40–60)	10.7%	11%
NaCl−UCl_3−$ThCl_4$	23.6%	23.2%
NaCl−UCl_3−UCl_4	10.35%	9.85%

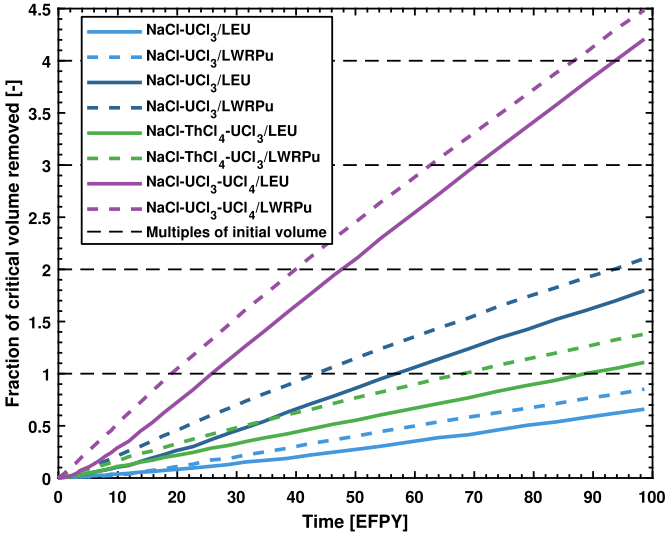

Fig. 11. Evolution of the cumulative volume of fuel salt discharged during the transition to equilibrium.

Table 4. First doubling times for candidate salts as function of the start-up fuel.

Doubling time [EFPY]	LEU	LWRPu
NaCl−UCl_3 (32–68)	142	113
NaCl−UCl_3 (40–60)	56.8	43.3
NaCl−UCl_3−$ThCl_4$	88.6	68
NaCl−UCl_3−UCl_4	25.8	19

5.3 Start-up inventory

For the initial core load, both enriched uranium and Light Water Reactor Plutonium (LWRPu) were considered. The LWRPu composition was chosen to represent LWR fuel discharged at a burn-up of 60 GWd/t: 3.1% ^{238}Pu, 52.5% ^{239}Pu, 24.6% ^{240}Pu, 12.2% ^{241}Pu and 7.7% ^{242}Pu. In the first case, the enrichment was varied so as to achieve criticality. In the second case, the quantity of LWRPu was varied to obtain a critical configuration, the rest of the actinide vector being composed of ^{238}U. In the case of the Th-containing salt, half of the actinide vector is composed of ^{232}Th.

Table 5. Reactivity coefficients of selected salts at BOL and equilibrium in pcm/K.

	Doppler			Density			Total		
	BOL		EQL	BOL		EQL	BOL		EQL
Salt	LEU	LWRPu		LEU	LWRPu		LEU	LWRPu	
$NaCl-UCl_3$ (32–68)	−1.2	−1.3	−0.9	−3.7	−2.8	−3.9	−4.9	−4.1	−4.8
$NaCl-UCl_3$ (40–60)	−0.3	−0.9	−4.6	−4.9	−4.3	−8.9	−5.2	−5.3	−13.4
$NaCl-UCl_3-ThCl_4$	−0.6	−0.3	−7.0	−6.6	−4.1	−8.1	−7.2	−4.4	−15.1
$NaCl-UCl_3-UCl_4$	−0.4	−0.8	−6.1	−13.2	−13.6	−15.9	−13.6	−14.4	−22.0

5.4 Doubling time

In the transition to equilibrium, reactivity is controlled by discharging slightly supercritical fuel and replacing it with fertile feed. Therefore, once the cumulative volume of fuel discharged reaches the initial equilibrium critical volume, and additional initial inventory has been bred. The time needed to reach this point is the doubling time of the reactor. It is depicted in Figure 11.

More actinide-dense salts improve the doubling time substantially over less dense salts and a LWRPu start-up results in a lower doubling time than a LEU start-up.

5.5 Reactivity coefficients

In an homogeneous fast-spectrum MSR, the main reactivity feedback is that of fuel salt expansion with higher temperature, which expels fissile nuclides out of the core and into an expansion tank, thereby lowering reactivity.

The reactivity coefficient α can be calculated using the following equation:

$$\alpha = \frac{\Delta\rho}{\Delta T} = 10^5 \frac{1}{T_{\text{hot}} - T_{\text{nom}}} \left(\frac{1}{k_{\text{nom}}} - \frac{1}{k_{\text{hot}}} \right) \qquad (9)$$

in which T_{nom} and k_{nom} are the nominal temperature and multiplication factor and T_{hot} and k_{hot} the temperature and multiplication factor at higher temperature.

Reactivity coefficients were computed at BOL and EQL using (9) by increasing the temperature of the cross-section library by 300 K for the Doppler coefficient and decreasing the density to that computed for the new temperature using (8) for the Density coefficient. They are summarized in Table 5.

It is clear that the reactivity coefficients are negative for all cases and increase (in absolute value) between BOL and EQL. Salts with higher actinide chloride densities result in cores with more negative density reactivity coefficients but lower Doppler coefficients due to spectrum hardening.

6 Conclusion

The feasibility of using a BNB fuel cycle in single-fluid molten salt reactors was investigated from a neutronics and fuel cycle point of view. The investigations presented in this paper show that BNB is indeed feasible in single-fluid molten salt reactors using a suitable salt composition and reflector material, provided that the salt used is chloride-based where the chlorine is enriched in ^{37}Cl. Several potential salt compositions were selected to further study, including their transition to equilibrium. The smallest reactor inventories are reached when using salts with high actinide densities. Burn-ups of 33–37% FIMA can be reached at the smallest core size.

The feasible core dimensions and volumes with most salts and reflector materials remain large (in the 100 m^3 range), however, compared to other molten salt reactor concepts. Alternative ways to operate a BNB MSR can be proposed, such as controlling excess reactivity from breeding using a different method (variable reflector, burnable poisons, control rods or neutronic feedbacks). However, they are likely to decrease the breeding capability of the system since they rely on decreasing the neutron budget of the reactor.

Moreover, the technical feasibility of the concept remains to be demonstrated from other points of view. Notably, the salt chemistry of chloride salt fuels has not been as investigated as well as that of fluoride fuels and which materials may be compatible with chlorides containing fission products has not been well established. The large burn-up that needs to be achieved results in high fission product concentrations in the salt despite the removal of volatile and insoluble fission products. Notably, substantial amounts of lanthanides are expected to remain in the salt. Their effect on the melting point of the salt mixture must be investigated to ensure that no precipitation of elements takes place during reactor operation. The feasibility of chlorine enrichment to the high levels necessary to obtain a small enough inventory must also be confirmed.

The authors gratefully acknowledge the support of the Swiss National Science Foundation (SNSF) grant number 152612 and a grant of the Project and Research Fund (PSEL) of the Association of Swiss Electricity Producers (VSE).

Author contribution statement

Boris Hombourger has performed the calculations and written the article. Jiri Krepel and Andreas Pautz have contributed to this work by providing support through expert judgement, critical verification, and proofreading on the various elements of this article.

Nomenclature

Acronyms

RTD	residence time distribution
SWR	standing wave reactor
TWR	traveling wave reactor
BNB	breed-and-burn
MSR	molten salt reactor
MSFR	molten salt fast reactor
LWRPu	light water reactor plutonium
FP	fission product
ORNL	Oak Ridge National Laboratory
LEU	low-enriched uranium
HEU	high-enriched uranium
BOL	beginning-of-life
EQL	equilibrium
GIF	generation IV international forum
EVOL	evaluation and viability of liquid fuel fast reactor system
CSTR	continuously-stirred tank reactor
FIMA	fissions per initial metal atom
SFR	sodium-cooled fast reactor

Symbols

k_∞	infinite multiplication factor
$\overline{\nu}$	average number of neutrons per fission
ϕ	scalar neutron flux
ρ	density
Σ_a	absorption macroscopic cross-section
Σ_f	fission macroscopic cross-section
τ	discharge cycle time

References

1. S.M. Feinberg, E.P. Kunegin, Discussion Comments, in *Proceedings of the Second United Nations International Conference on the Peaceful Uses of Atomic Energy* (International Atomic Energy Agency, Geneva, Switzerland, 1958), Vol. 9, pp. 446–447
2. K. Fuchs, H. Hessel, über die Möglichkeiten des Betriebs eines Natururanbrutreaktors ohne Brennstoffaufbereitung, Kernenergie **4**, 619 (1961)
3. E. Teller, M. Ishikawa, L. Wood, Completely automated nuclear power reactors for long-term operation, in *Proceedings of the Frontier in Physics Symposium, Lubbock, TX, USA, 1995*
4. H. Sekimoto, K. Ryu, Y. Yoshimura, CANDLE: The New Burnup Strategy, Nucl. Sci. Eng. **139**, 306 (2001)
5. P. Hejzlar, R. Petroski, J. Cheatham, N. Touran, M. Cohen, B. Truong, R. Latta, M. Werner, T. Burke, J. Tandy, M. Garrett, B. Johnson, T. Ellis, J. Mcwhirter, A. Odedra, P. Schweiger, D. Adkisson, J. Gilleland, Terrapower, LLC Traveling wave reactor development program overview, Nucl. Eng. Technol. **45**, 731 (2013)
6. R. Lopez-Solis, J.-L. François, The breed and burn nuclear reactor: a chronological, conceptual, and technological review, Int. J. Energy Res., https://doi.org/10.1002/er.3854
7. S. Qvist, J. Hou, E. Greenspan, Design and performance of 2D and 3D-shuffled breed-and-burn cores, Ann. Nucl. Energy **85**, 93 (2015)
8. B. Hombourger, J. Křepel, K. Mikityuk, A. Pautz, Fuel Cycle Analysis of a Molten Salt Reactor for Breed-and-Burn Mode, in *Proceedings of the 2015 International Congress on Advances in Nuclear Power Plants* (Société Française d'Énergie Nucléaire, Nice, France, 2015)
9. B. Hombourger, J. Křepel, K. Mikityuk, A. Pautz, On the Feasibility of Breed-and-Burn Fuel Cycles in Molten Salt Reactors, in *Proceedings of FR17. International Atomic Energy Agency, Yekaterinburg, Russian Federation, 2017*
10. M. Martin, M. Aufiero, E. Greenspan, M. Fratoni, Feasibility of a Breed-and-Burn Molten Salt Reactor, in *Proceedings of ICAPP '17* (American Nuclear Society, San Francisco, CA, USA, 2017)
11. A. Kasam, E. Shwageraus, Feasibility studies of a Breed and Burn Molten Salt Reactor, in *Proceedings of ICAPP 2017* (Atomic Energy Society of Japan, Fukui and Kyoto, Japan, 2017)
12. I. Scott, 21 - Stable salt fast reactor, in *Molten Salt Reactors and Thorium Energy*, edited by T.J. Dolan (Woodhead Publishing, 2017), pp. 571–580
13. F. Heidet, E. Greenspan, Neutron Balance Analysis for Sustainability of Breed-and-Burn Reactors, Nucl. Sci. Eng. **171**, 13 (2012)
14. R. Petroski, B. Forget, C. Forsberg, Using the Neutron Excess Concept to Determine Starting Fuel Requirements for Minimum Burnup Breed-and-Burn Reactors, Nucl. Technol. **175**, 388 (2011)
15. P.V. Danckwerts, Continuous flow systems: Distribution of residence times, Chem. Eng. Sci. **2**, 1 (1953)
16. B. Hombourger, J. Křepel, K. Mikityuk, A. Pautz, The EQL0D procedure for fuel cycle studies in molten salt reactors, in *Proceedings of the 2016 International Congress on Advances in Nuclear Power Plants* (American Nuclear Society, San Francisco, CA, USA, 2006)
17. J. Leppänen, M. Pusa, T. Viitanen, V. Valtavirta, T. Kaltiaisenaho, The Serpent Monte Carlo code: Status, development and applications in 2013, Ann. Nucl. Energy **82**, 142 (2015)
18. M. Pusa, Rational Approximations to the Matrix Exponential in Burnup Calculations, Nucl. Sci. Eng. **169**, 155 (2011)
19. W.R. Grimes, Reactor Chemistry Division Annual Progress Report For Period Ending December 31, 1965. Annual Progress Report ORNL-3913, Oak Ridge National Laboratory, Oak Ridge, TN, USA, 1966
20. E.H. Ottewitte, Configuration of a Molten Chloride Fast Reactor on a Thorium Fuel Cycle to Current Nuclear Fuel Cycle Concerns. Ph.D. Thesis, University of Californa in Los Angeles (UCLA), Los Angeles, CA, USA, 1982
21. O. Beneš, R. Konings, Thermodynamic evaluation of the NaCl–$MgCl_2$–UCl_3–$PuCl_3$ system, J. Nucl. Mater. **375**, 202 (2008)
22. R.C. Robertson, Conceptual Design Study of a Single-fluid Molten-salt Breeder Reactor. Report ORNL-4541 (Oak Ridge National Laboratory, Oak Ridge, TN, USA, 1971)

Cite this article as: Boris Hombourger, Jiři Křepel and Andreas Pautz. Breed-and-burn fuel cycle in molten salt reactors, EPJ Nuclear Sci. Technol. **5**, 15 (2019)